LABORATOIRE ONDES et MILIEUX COMPLEXES

UNIVERSITÉ LE HAVRE NORMANDIE

CNR NANOTEC INSTITUTE OF NANOTECHNOLOGY

UCL

State resolved cross sections and rate coefficients for electron-BeH^+, -BeD^+ and -BeT^+ collisions

Vincenzo Laporta

P.Las.M.I. lab, CNR-Nanotec, Bari (Italy)

Consultancy meeting on Be edge plasmas in fusion
IAEA 6-7 June 2019, Vienna, Vietnam

electron-BeH^+ and -BeD^+ state resolved cross sections

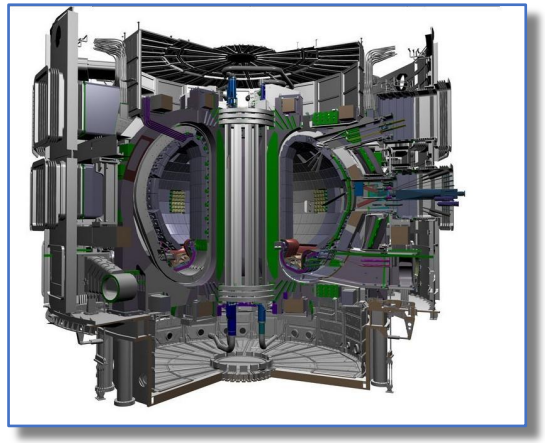

$$e + \mathrm{BeH}^+\left(\mathrm{X}\ ^1\Sigma^+; v, j\right) \rightarrow \begin{cases} \mathrm{BeH}^+\left(\mathrm{X}\ ^1\Sigma^+; v', j'\right) + e & (VE) \\ \mathrm{Be}^*(n = 1 \ldots 12) + \mathrm{H}\left(^2\mathrm{S}\right) & (DR) \\ \mathrm{Be}^+\left(^2\mathrm{S}\right) + \mathrm{H}\left(^2\mathrm{S}\right) + e & (DE) \\ \mathrm{BeH}^{+*} + e & (EE) \end{cases}$$

electron-BeH^+ and -BeD^+ state resolved cross sections

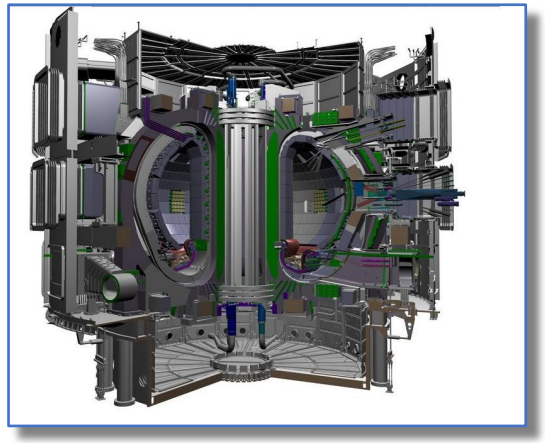

$$e + \mathrm{BeH}^+\left(\mathrm{X}\ ^1\Sigma^+; v, j\right) \rightarrow \begin{cases} \mathrm{BeH}^+\left(\mathrm{X}\ ^1\Sigma^+; v', j'\right) + e & (VE) \\ \mathrm{Be}^*(n = 1 \ldots 12) + \mathrm{H}\left(^2\mathrm{S}\right) & (DR) \\ \mathrm{Be}^+\left(^2\mathrm{S}\right) + \mathrm{H}\left(^2\mathrm{S}\right) + e & (DE) \\ \mathrm{BeH}^{+*} + e & (EE) \end{cases}$$

Potential energy curves and couplings

UK-R-Matrix

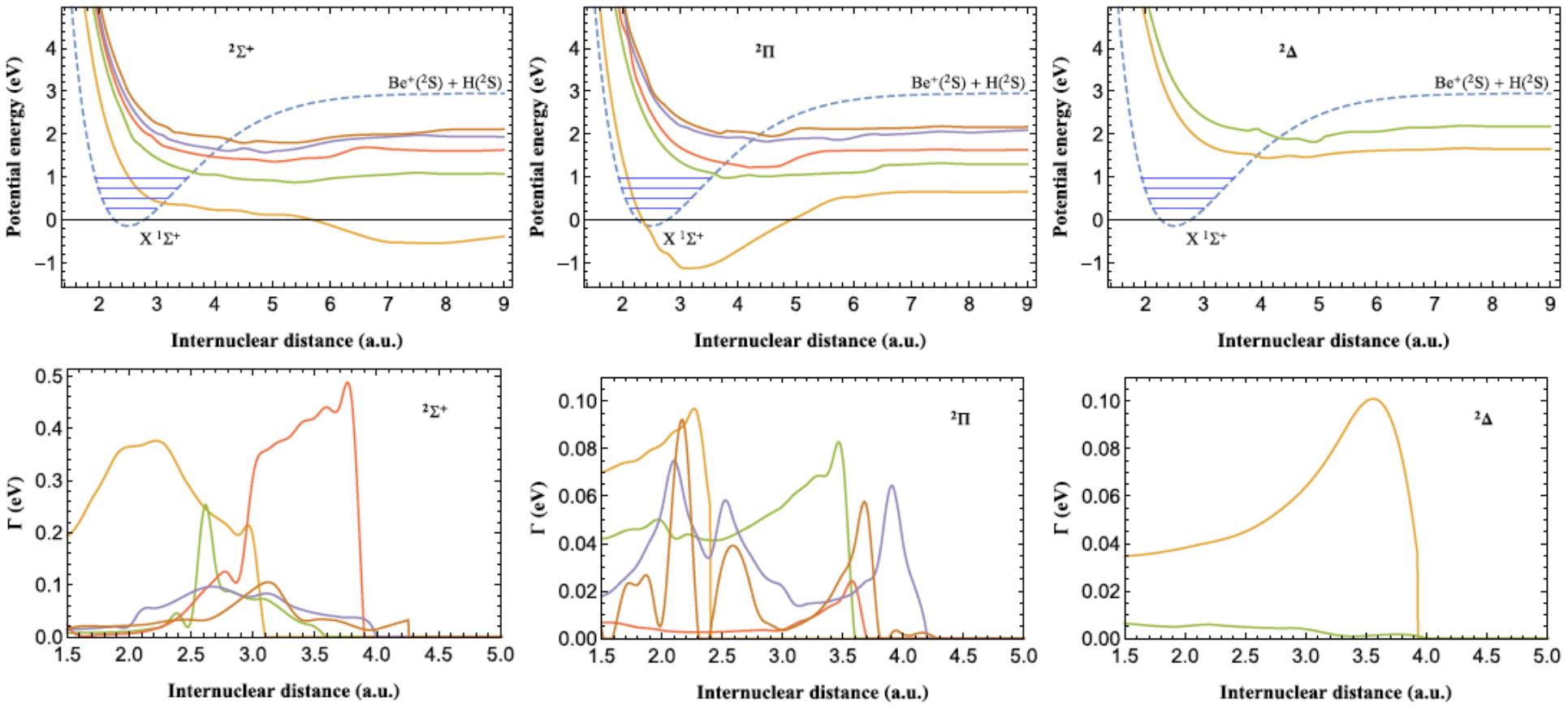

Figure 1. Potential energy curves (top line) and widths (bottom line) for BeH** resonant states in $^2\Sigma^+$, $^2\Pi$ and $^2\Delta$ scattering channels for $j^+ = 0$. Dashed line refers to potential energy curve for BeH^+ ground electronic state where the first vibrational levels are marked.

K Chakrabarti and J Tennyson J. Phys. B: At. Mol. Opt. Phys. 48 (2015) 235202
K Chakrabarti and J Tennyson Eur. Phys. J. D (2012) 66: 31

$$e + \mathrm{BeH}^+\left(\mathrm{X}\ ^1\Sigma^+; v, j\right) \rightarrow \mathrm{BeH}^+\left(\mathrm{X}\ ^1\Sigma^+; v', j'\right) + e$$

VE cross sections: comparison between
Configuration Interactions (CI)/R-Matrix and MQDT/Kohn methods

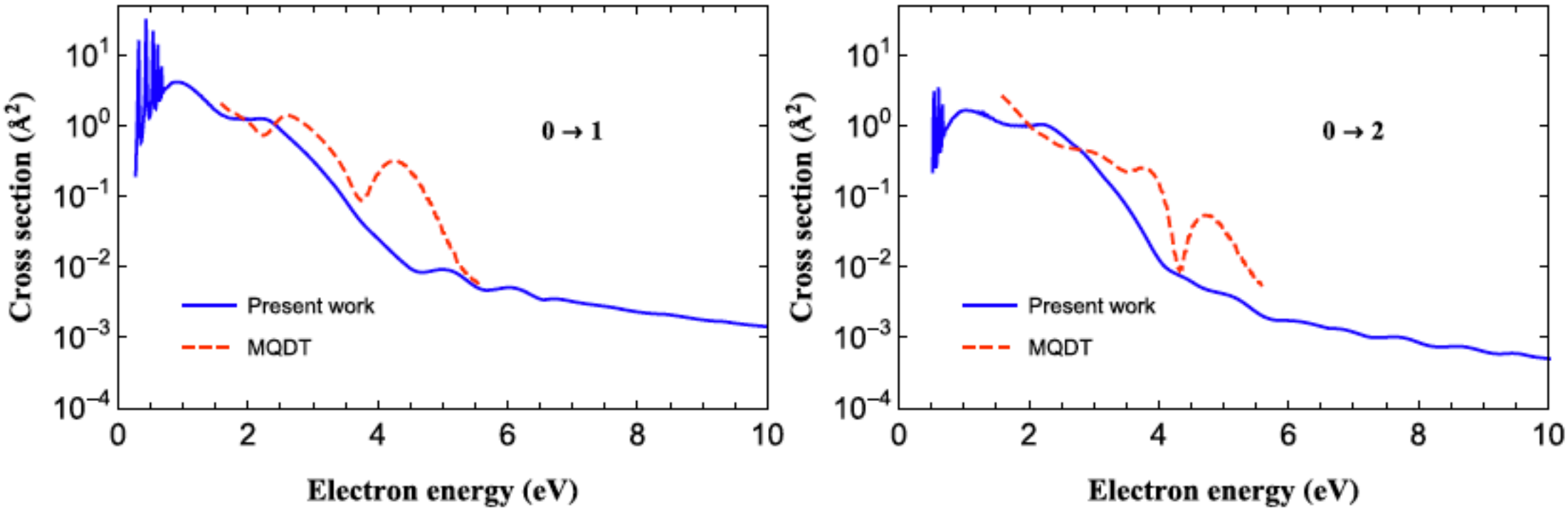

$$e + \mathrm{BeH}^+\left(\mathrm{X}\ ^1\Sigma^+; v, j\right) \rightarrow \mathrm{BeH}^+\left(\mathrm{X}\ ^1\Sigma^+; v', j'\right) + e$$

VE cross sections: comparison between
Configuration Interactions (CI)/R-Matrix and MQDT/Kohn methods

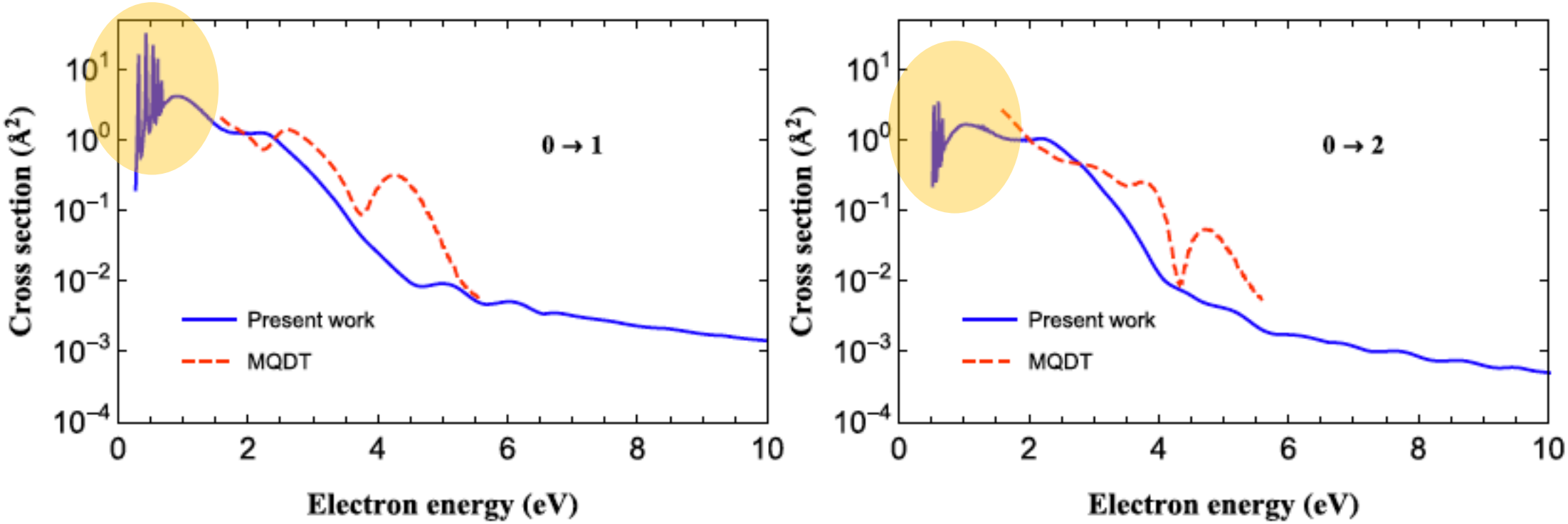

$$e + \mathrm{BeH}^{+}\left(\mathrm{X}\ ^{1}\Sigma^{+}; v, j\right) \rightarrow \mathrm{Be}^{*}(n = 1 \ldots 12) + \mathrm{H}\left(^{2}\mathrm{S}\right)$$

DR cross sections: comparison between
Configuration Interactions (CI)/R-Matrix and MQDT/Kohn methods

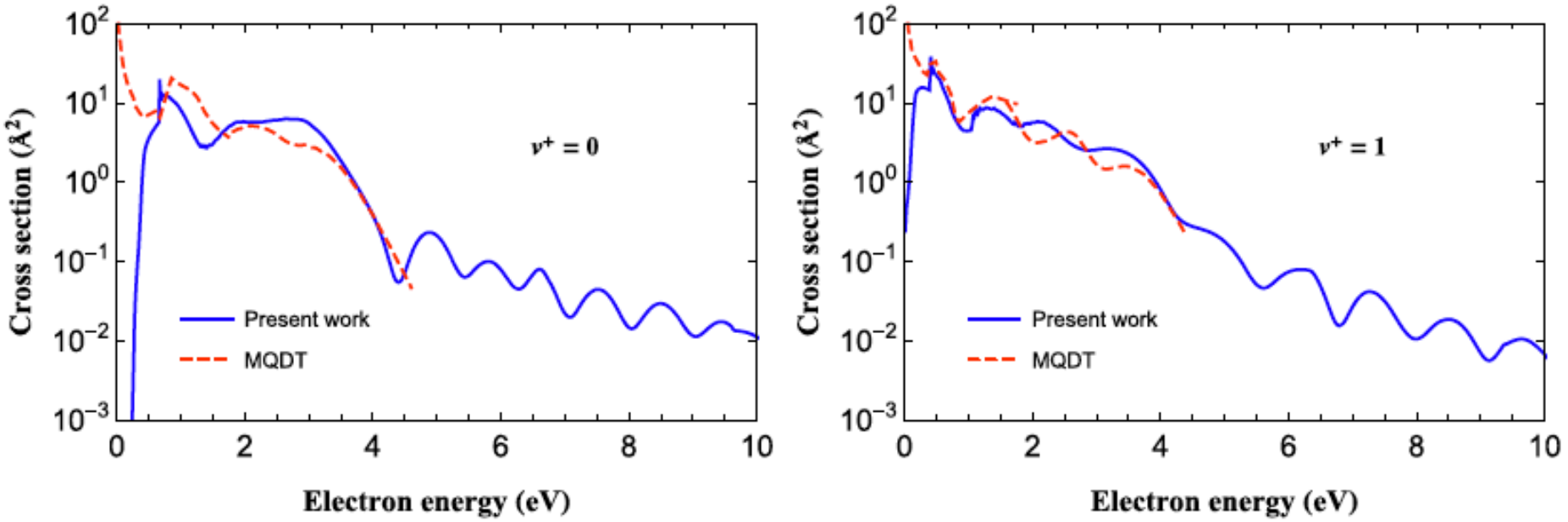

Figure 5. Dissociative recombination cross sections: comparison between the present calculations (full line) and MQDT/Kohn results [12] (dashed line).

$$e + \mathrm{BeH}^{+}\left(\mathrm{X}\,^{1}\Sigma^{+}; v, j\right) \rightarrow \mathrm{Be}^{*}(n = 1 \ldots 12) + \mathrm{H}\left(^{2}\mathrm{S}\right)$$

DR cross sections: comparison between
Configuration Interactions (CI)/R-Matrix and MQDT/Kohn methods

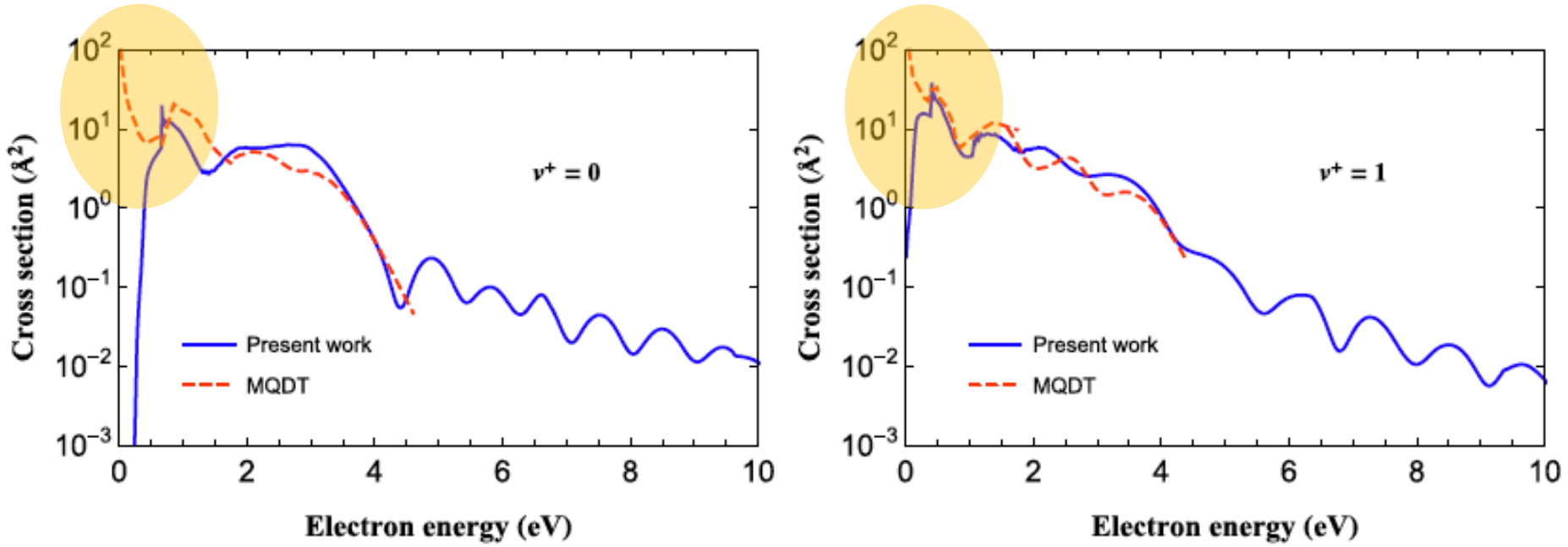

Figure 5. Dissociative recombination cross sections: comparison between the present calculations (full line) and MQDT/Kohn results [12] (dashed line).

$e + \mathrm{BeH}^+$

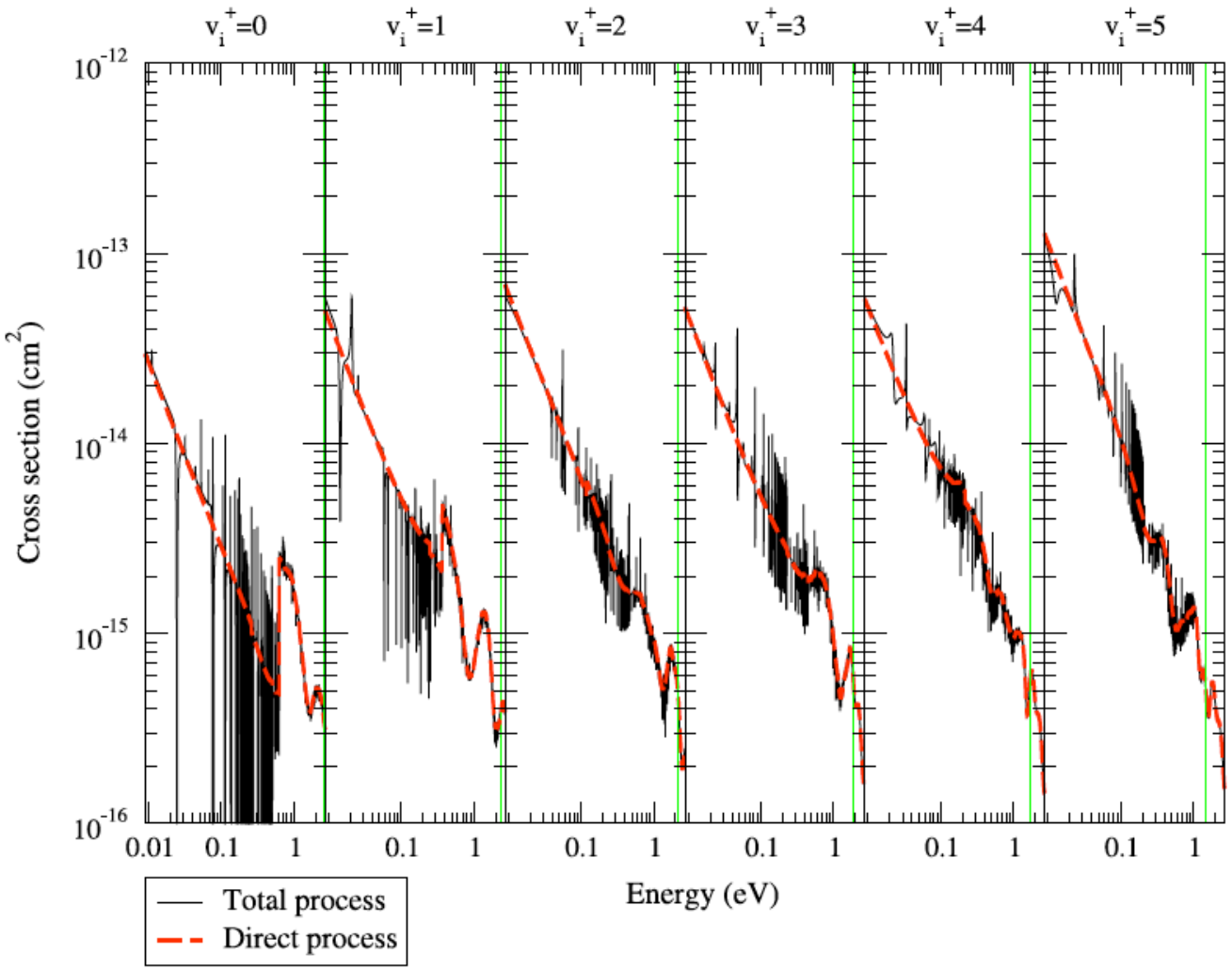
v_i^+=0
v_i^+=1
v_i^+=2
v_i^+=3
v_i^+=4
v_i^+=5
Cross section (cm^2)
10^-12
10^-13
10^-14
10^-15
10^-16
0.01
0.1
1
Energy (eV)
Total process
Direct process

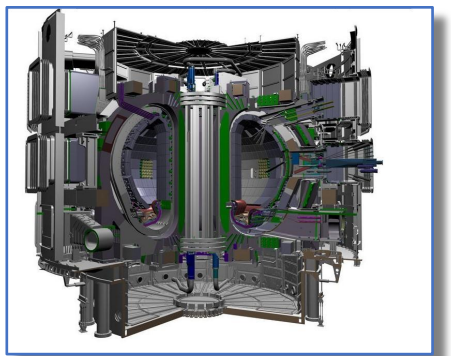

$e + \mathrm{BeH}^+$

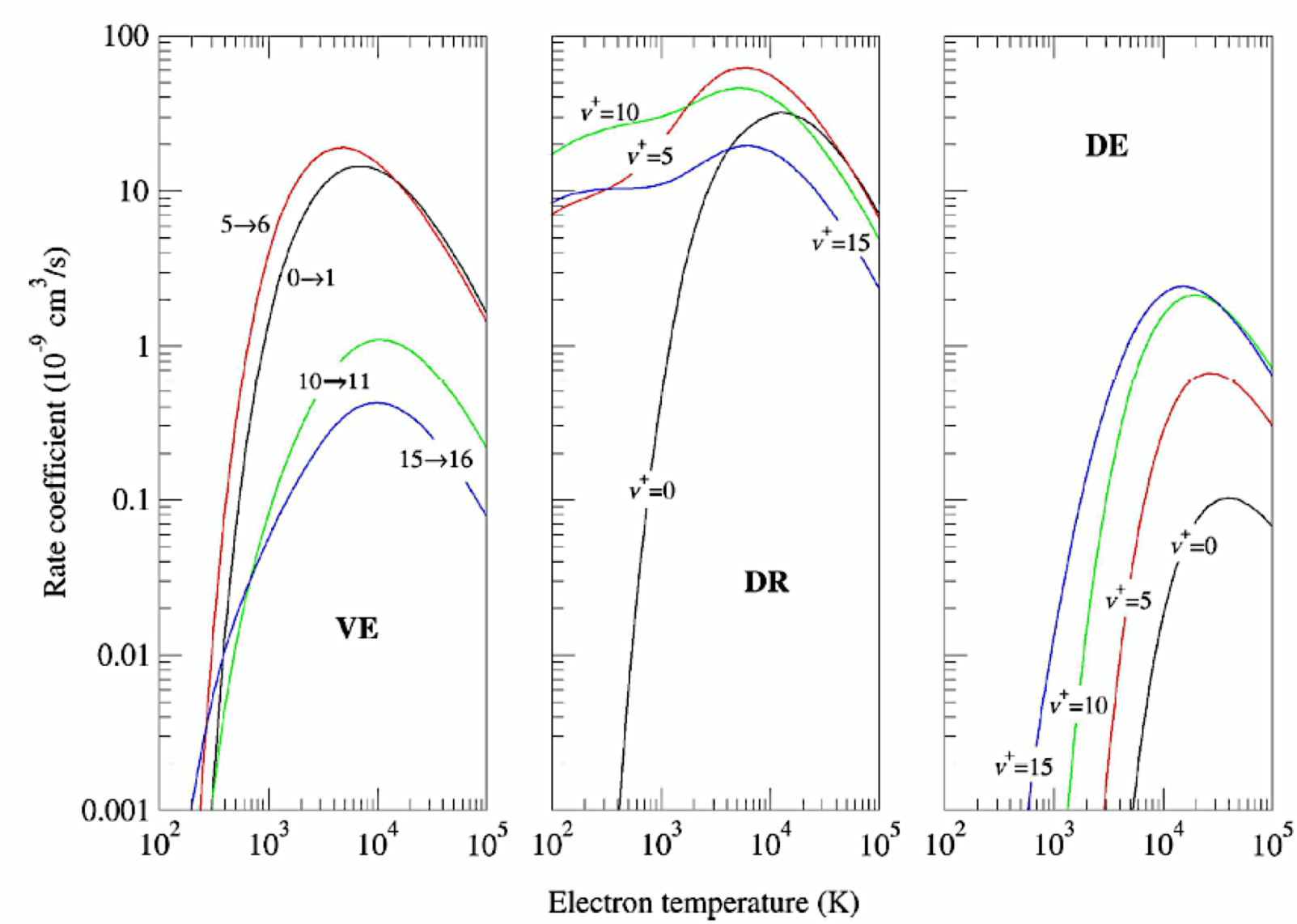
Rate coefficient (10^{-9} cm^3/s)
100
10
1
0.1
0.01
0.001
5→6
0→1
10→11
15→16
VE
v^+=10
v^+=5
v^+=15
v^+=0
DR
DE
v^+=0
v^+=5
v^+=10
v^+=15
10^2
10^3
10^4
10^5
Electron temperature (K)

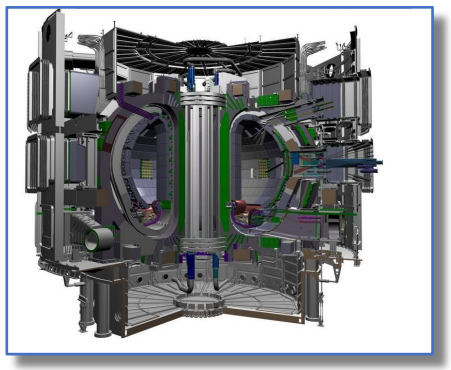

$e + \mathrm{BeD}^+$

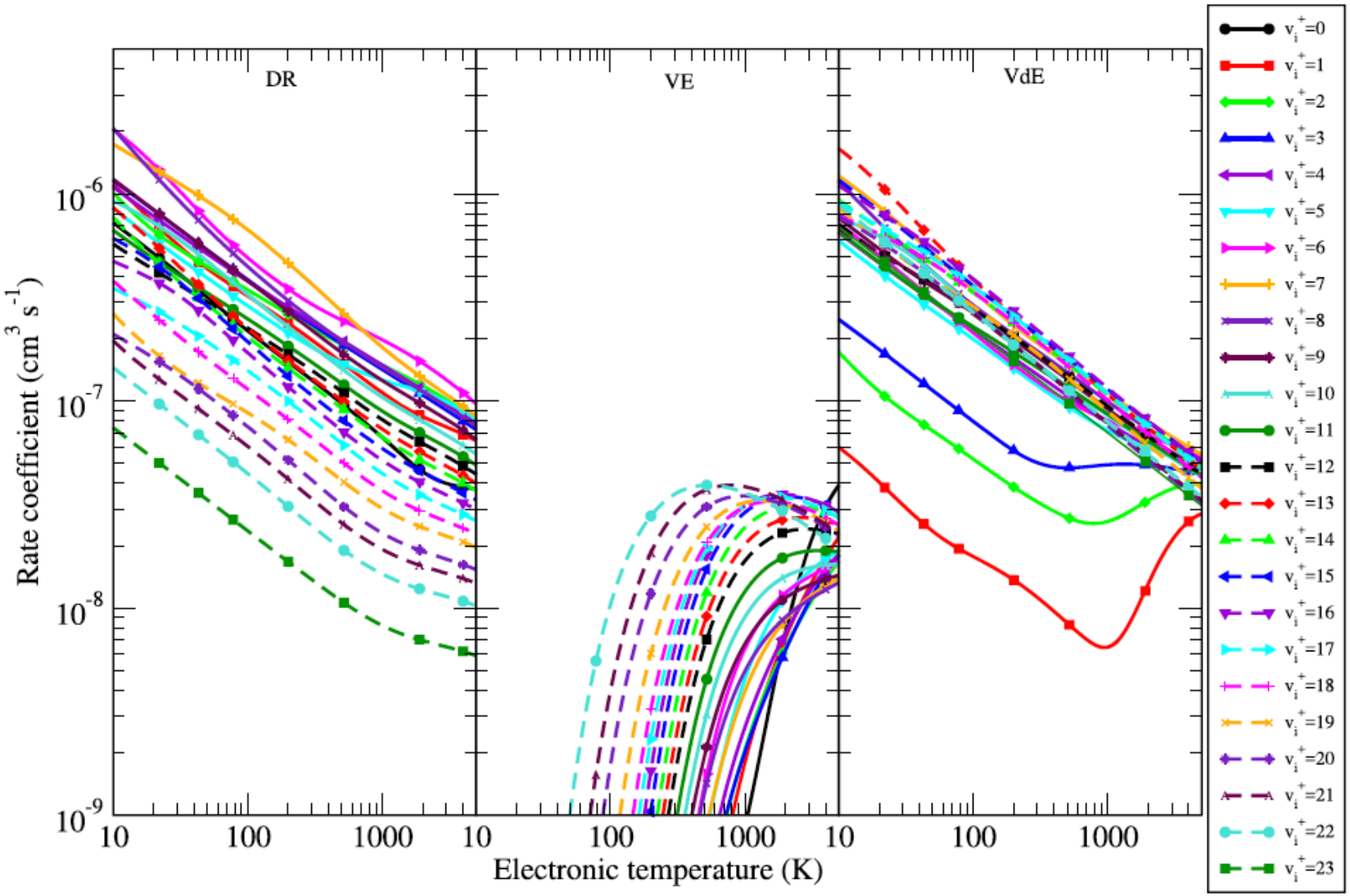
DR
VE
VdE
Rate coefficient (cm^3 s^{-1})
10^{-6}
10^{-7}
10^{-8}
10^{-9}
10
100
1000
Electronic temperature (K)
v_i^+=0
v_i^+=1
v_i^+=2
v_i^+=3
v_i^+=4
v_i^+=5
v_i^+=6
v_i^+=7
v_i^+=8
v_i^+=9
v_i^+=10
v_i^+=11
v_i^+=12
v_i^+=13
v_i^+=14
v_i^+=15
v_i^+=16
v_i^+=17
v_i^+=18
v_i^+=19
v_i^+=20
v_i^+=21
v_i^+=22
v_i^+=23

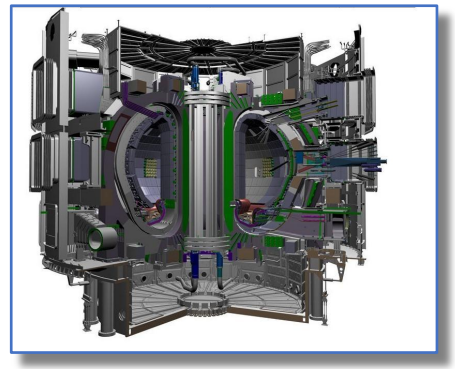

$e + \mathrm{BeT}^+$

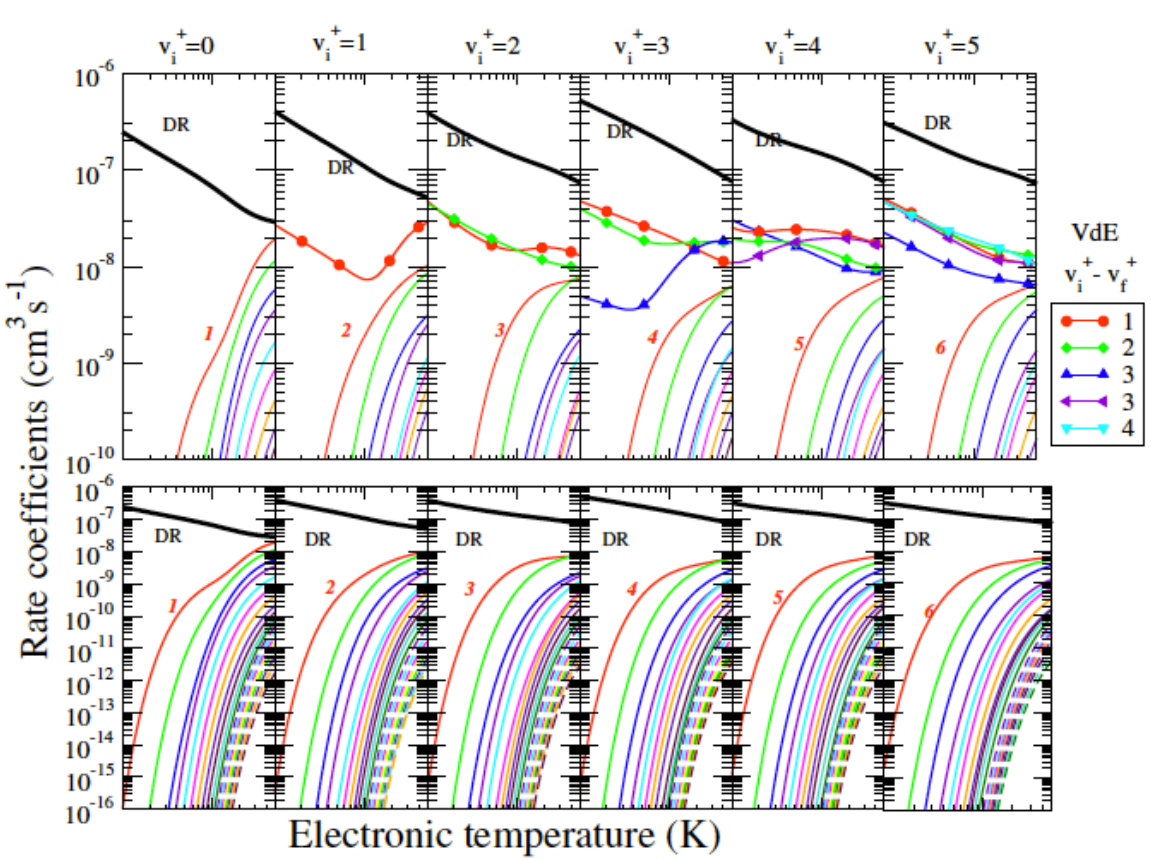

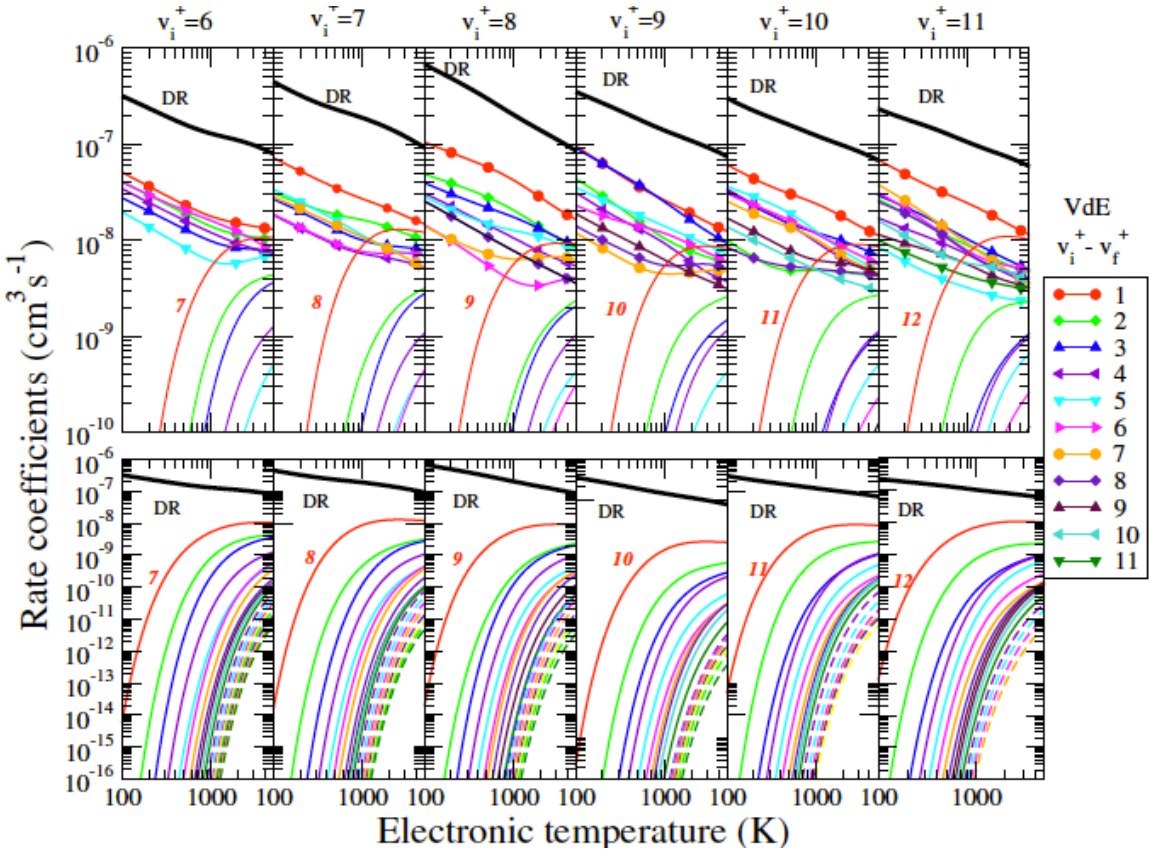

In preparation…

Global fit

$$k^{P}_{(BeH^{+},L)}(T_e) = A_L\, T_e^{\alpha_L}\, \exp\left[-\sum_{j=1}^{7} \frac{B_L(j)}{j\, T_e^{j}}\right],$$

List of the parameters used in Eq. (10) for the DR Maxwell rate coefficients of $BeH^{+}(v_i^{+} = 0, 1, 2, 3, \ldots, 17)$ displayed in Graphs 4–6.

v_i^+	$A_{v_i^+}$	$\alpha_{v_i^+}$	$B_{v_i^+}(1)$	$B_{v_i^+}(2)$	$B_{v_i^+}(3)$	$B_{v_i^+}(4)$	$B_{v_i^+}(5)$	$B_{v_i^+}(6)$	$B_{v_i^+}(7)$
0	$0.253513120 \times 10^{-9}$	0.592469479	$-0.19064941 \times 10^{4}$	0.12331500×10^{7}	$-0.38834250 \times 10^{9}$	$0.64726558 \times 10^{11}$	$-0.56672264 \times 10^{13}$	$0.23206898 \times 10^{15}$	$-0.29507881 \times 10^{16}$
1	$0.31446233 \times 10^{-5}$	−0.407538250	0.95857771×10^{3}	$-0.13595793 \times 10^{7}$	0.72543620×10^{9}	$-0.19264094 \times 10^{12}$	$0.27181254 \times 10^{14}$	$-0.19476594 \times 10^{16}$	$0.55722181 \times 10^{17}$
2	$0.11467872 \times 10^{-5}$	−0.322376187	$-0.26563039 \times 10^{3}$	0.21960169×10^{6}	$-0.91654913 \times 10^{8}$	$0.20725586 \times 10^{11}$	$-0.25961356 \times 10^{13}$	$0.16939687 \times 10^{15}$	$-0.44907404 \times 10^{16}$
3	$0.84964155 \times 10^{-6}$	−0.275140774	0.17167335×10^{3}	$-0.45195658 \times 10^{6}$	0.28509653×10^{9}	$-0.82740349 \times 10^{11}$	$0.12358875 \times 10^{14}$	$-0.92168032 \times 10^{15}$	$0.27161235 \times 10^{17}$
4	$.12123963 \times 10^{-04}$	$-.55584500 \times 10^{00}$	$.76129456 \times 10^{03}$	$-.71435106 \times 10^{06}$	$.30207319 \times 10^{09}$	$-.68762171 \times 10^{11}$	$.86945412 \times 10^{13}$	$-.57415087 \times 10^{15}$	$.15426341 \times 10^{17}$
5	$.64413939 \times 10^{-05}$	$-.49848174 \times 10^{00}$	$-.23877415 \times 10^{03}$	$.25006568 \times 10^{06}$	$-.10783678 \times 10^{09}$	$.24554732 \times 10^{11}$	$-.30939272 \times 10^{13}$	$.20355081 \times 10^{15}$	$-.54518844 \times 10^{16}$
6	$.79292741 \times 10^{-05}$	$-.53226218 \times 10^{00}$	$.33351152 \times 10^{03}$	$-.14850129 \times 10^{06}$	$.17170887 \times 10^{08}$	$.30513319 \times 10^{10}$	$-.99838927 \times 10^{12}$	$.95173683 \times 10^{14}$	$-.31443182 \times 10^{16}$
7	$.31608289 \times 10^{-05}$	$-.46404421 \times 10^{00}$	$.37872750 \times 10^{03}$	$-.42935055 \times 10^{06}$	$.20957344 \times 10^{09}$	$-.53972002 \times 10^{11}$	$.75540694 \times 10^{13}$	$-.54165315 \times 10^{15}$	$.15558026 \times 10^{17}$
8	$.12772097 \times 10^{-05}$	$-.37368620 \times 10^{00}$	$.15244133 \times 10^{03}$	$-.31635974 \times 10^{06}$	$.19418973 \times 10^{09}$	$-.56429439 \times 10^{11}$	$.84734597 \times 10^{13}$	$-.63481101 \times 10^{15}$	$.18769614 \times 10^{17}$
9	$.74656385 \times 10^{-06}$	$-.32403101 \times 10^{00}$	$.60281855 \times 10^{02}$	$-.26426288 \times 10^{06}$	$.18271539 \times 10^{09}$	$-.55697834 \times 10^{11}$	$.85696766 \times 10^{13}$	$-.65123675 \times 10^{15}$	$.19433329 \times 10^{17}$
10	$.94813785 \times 10^{-06}$	$-.38179684 \times 10^{00}$	$.93138403 \times 10^{02}$	$-.20887005 \times 10^{06}$	$.13764353 \times 10^{09}$	$-.41661584 \times 10^{11}$	$.64143533 \times 10^{13}$	$-.48869838 \times 10^{15}$	$.14625021 \times 10^{17}$
11	$.56313061 \times 10^{-06}$	$-.32311526 \times 10^{00}$	$-.77607252 \times 10^{02}$	$-.17424595 \times 10^{05}$	$.40844169 \times 10^{08}$	$-.15764324 \times 10^{11}$	$.26801483 \times 10^{13}$	$-.21496788 \times 10^{15}$	$.66320236 \times 10^{16}$
12	$.35708859 \times 10^{-06}$	$-.29280901 \times 10^{00}$	$-.17138479 \times 10^{03}$	$.63705373 \times 10^{05}$	$.33130264 \times 10^{06}$	$-.52225664 \times 10^{10}$	$.12088046 \times 10^{13}$	$-.11033839 \times 10^{15}$	$.36564426 \times 10^{16}$
13	$.23814658 \times 10^{-06}$	$-.26653146 \times 10^{00}$	$-.14902427 \times 10^{03}$	$.45030050 \times 10^{04}$	$.37246513 \times 10^{08}$	$-.15455621 \times 10^{11}$	$.26689680 \times 10^{13}$	$-.21509204 \times 10^{15}$	$.66474458 \times 10^{16}$
14	$.16822148 \times 10^{-06}$	$-.24834680 \times 10^{00}$	$-.68663615 \times 10^{02}$	$-.13388071 \times 10^{06}$	$.10834629 \times 10^{09}$	$-.33601161 \times 10^{11}$	$.51515738 \times 10^{13}$	$-.38888760 \times 10^{15}$	$.11532273 \times 10^{17}$
15	$.96311475 \times 10^{-07}$	$-.22323807 \times 10^{00}$	$-.44467944 \times 10^{02}$	$-.18367203 \times 10^{06}$	$.13171836 \times 10^{09}$	$-.38871744 \times 10^{11}$	$.57918282 \times 10^{13}$	$-.42923231 \times 10^{15}$	$.12567765 \times 10^{17}$
16	$.10223003 \times 10^{-06}$	$-.26775897 \times 10^{00}$	$.18549236 \times 10^{03}$	$-.40254132 \times 10^{06}$	$.23043174 \times 10^{09}$	$-.63092045 \times 10^{11}$	$.90757284 \times 10^{13}$	$-.65955762 \times 10^{15}$	$.19077977 \times 10^{17}$
17	$.34252448 \times 10^{-07}$	$-.21655952 \times 10^{00}$	$.79722891 \times 10^{02}$	$-.30691665 \times 10^{06}$	$.19188108 \times 10^{09}$	$-.54737984 \times 10^{11}$	$.80633597 \times 10^{13}$	$-.59496368 \times 10^{15}$	$.17389215 \times 10^{17}$

S. Niyonzima, I. F. Schneider et al., PHYSICAL REVIEW A 87, 022713 (2013)
*V. Laporta, K. Chakrabarti, et al., Plasma Phys. Control. Fusion **59**, 045008 (2017)*
***S. Niyonzima, I. F. Schneider et al.,** Atomic Data and Nuclear Data Tables 115–116 (2017) 287–308*
*S. Niyonzima, V. Laporta, et al., Plasma Sources Sci. Technol. **27**, 025015 (2018)*
S Niyonzima, N Pop et al. Plasma Sources Sci. Technol. 27 (2018) 025015
N. Pop et al in preparation (2019)

electron-BeH^+ and -BeD^+ state resolved cross sections

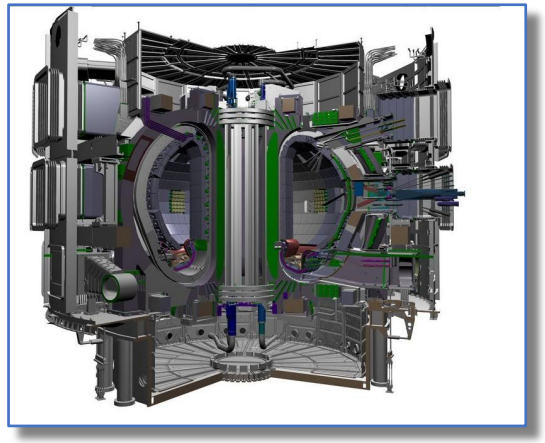

$$e + \mathrm{BeH}^+\left(\mathrm{X}\ ^1\Sigma^+; v, j\right) \rightarrow \begin{cases} \mathrm{BeH}^+\left(\mathrm{X}\ ^1\Sigma^+; v', j'\right) + e & (VE) \\ \mathrm{Be}^*(n = 1 \ldots 12) + \mathrm{H}\left(^2\mathrm{S}\right) & (DR) \\ \mathrm{Be}^+\left(^2\mathrm{S}\right) + \mathrm{H}\left(^2\mathrm{S}\right) + e & (DE) \\ \mathrm{BeH}^{+*} + e & (EE) \end{cases}$$

UK-R-Matrix

BeH^+ potential energy curves

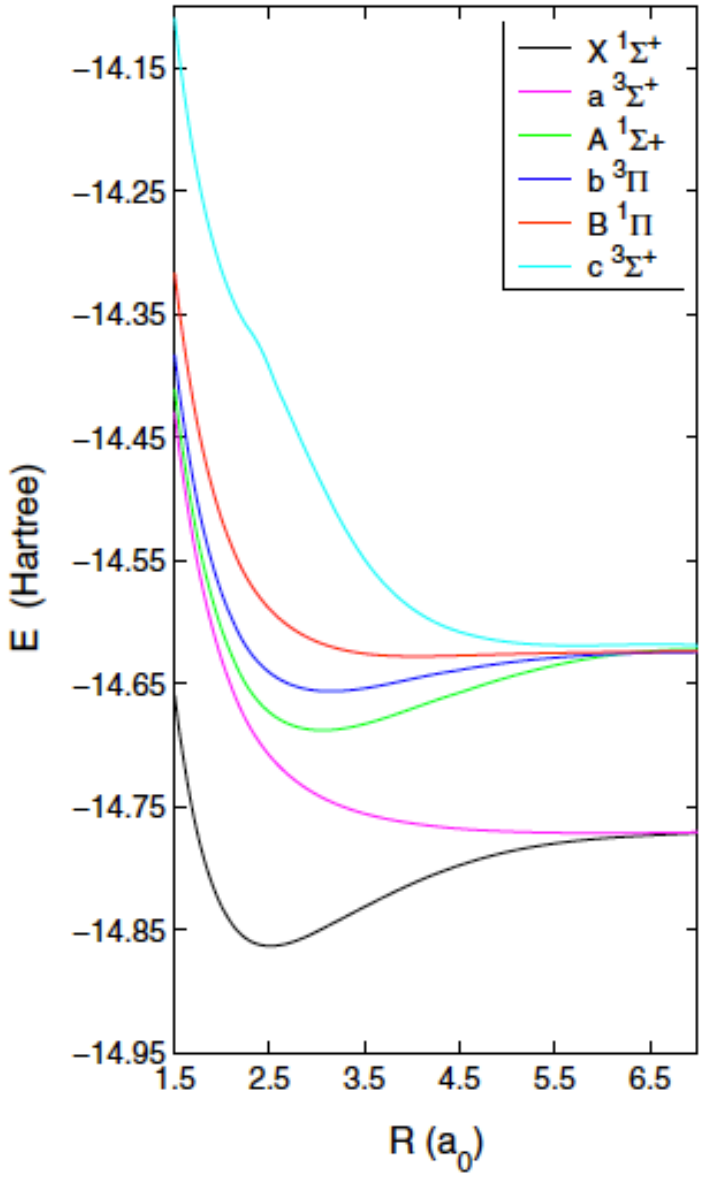

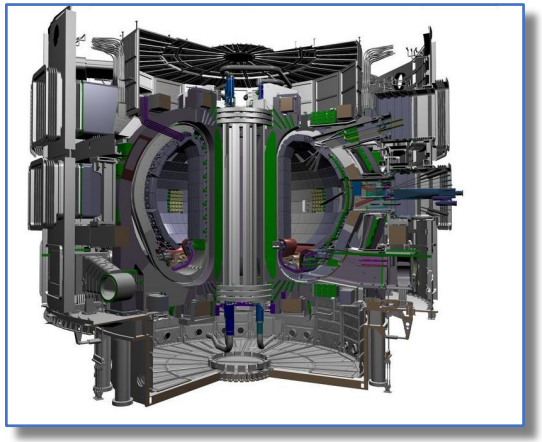

K Chakrabarti and J Tennyson J. Phys. B: At. Mol. Opt. Phys. 48 (2015) 235202
K Chakrabarti and J Tennyson Eur. Phys. J. D (2012) 66: 31

$e + He_2^+$ collisions

$$e + He_2^+(X\ ^2\Sigma_u^+, v = 0 - 23) \rightarrow e + He_2^+(A\ ^2\Sigma_g^+) \rightarrow e + He + He^+,$$

R Celiberto, KL Baluja, RK Janev and V Laporta, Plasma Phys. Control. Fusion 58 (2015) 014024

electron-He_2^+ dissociation cross sections

$$e + He_2^+(X\ ^2\Sigma_u^+, v = 0 - 23) \rightarrow e + He_2^+(A\ ^2\Sigma_g^+) \rightarrow e + He + He^+,$$

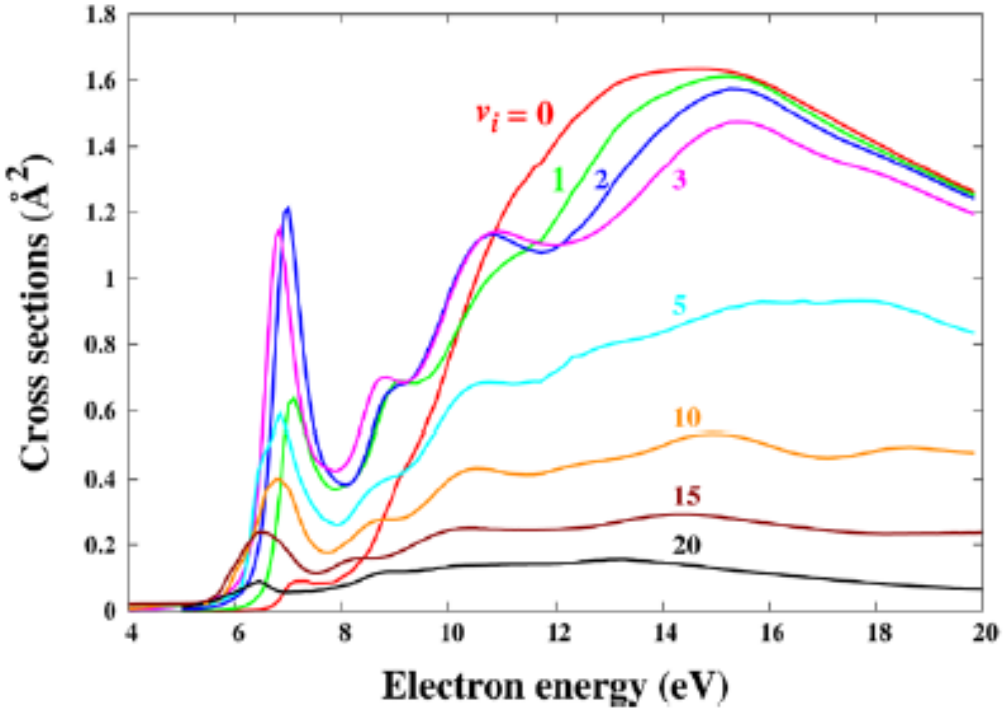

Figure 4. AN cross sections for processes starting from different He_2^+ vibrational levels v.

R Celiberto, KL Baluja, RK Janev and V Laporta, Plasma Phys. Control. Fusion 58 (2015) 014024

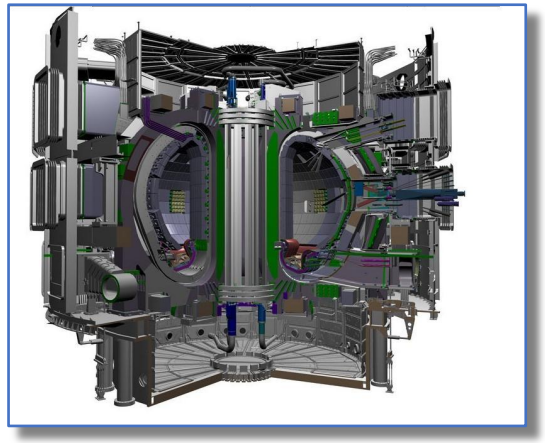

Thank you for your attention…

Electronic excitation cross sections @ $R = 2.5369\ a_0$

UK-R-Matrix

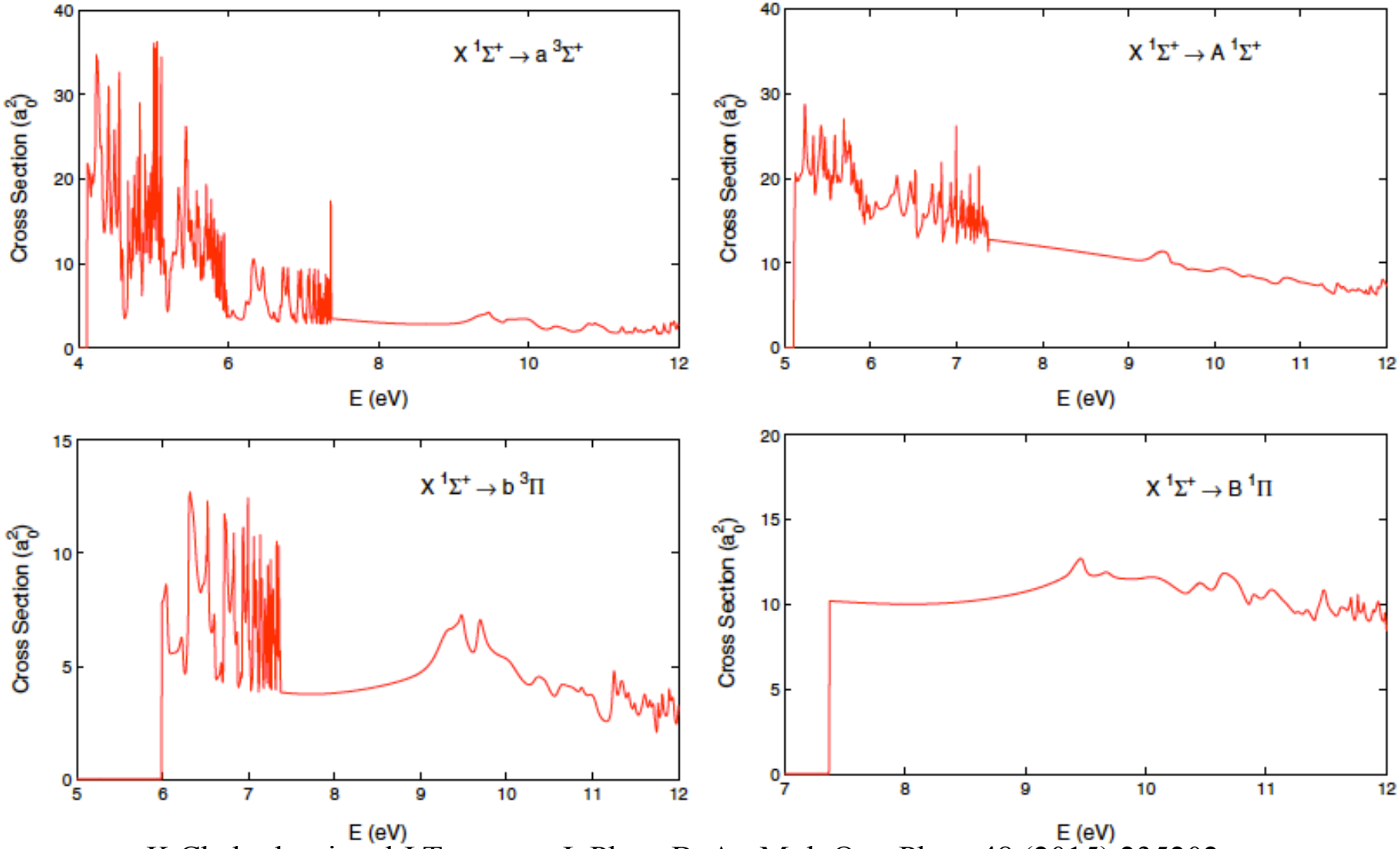

K Chakrabarti and J Tennyson J. Phys. B: At. Mol. Opt. Phys. 48 (2015) 235202
K Chakrabarti and J Tennyson Eur. Phys. J. D (2012) 66: 31